

# Conformational Studies by Dynamic NMR. 89.<sup>1</sup> Stereomutation and Cryogenic Enantioseparation of Conformational Antipodes of Hindered Aryl Oximes

Francesco Gasparri,<sup>\*,†</sup> Stefano Grilli,<sup>‡</sup> Rino Leardini,<sup>‡</sup> Lodovico Lunazzi,<sup>\*,‡</sup>  
Andrea Mazzanti,<sup>‡</sup> Daniele Nanni,<sup>‡</sup> Marco Pierini,<sup>§</sup> and Marco Pinamonti<sup>‡</sup>

Department of Organic Chemistry "A. Mangini", University of Bologna, Viale Risorgimento, 4, Bologna 40136, Italy, Dipartimento di Chimica Tecnologia delle Sostanze Biologicamente Attive, Università "La Sapienza", P.le A. Moro, 5, Roma 00185, Italy, and Dipartimento Scienze del Farmaco, Università "G. D'Annunzio", Chieti 66013, Italy

lunazzi@ms.fci.unibo.it

Received January 21, 2002

Aryl benzyl oximes having the configuration *Z* give rise to stereolabile atropisomers when a halogen atom is present in the ortho position of the aryl moiety, as a consequence of the restricted aryl–CN bond rotation. By means of dynamic <sup>1</sup>H NMR spectroscopy it has been possible to determine the corresponding rotation barrier, hence the lifetime of the atropisomers that, in the case of the iodine derivative, was found sufficiently long as to allow a physical separation to be achieved on an appropriately cooled enantioselective HPLC column. Comparison of the barriers determined by dynamic NMR and dynamic HPLC proved the equivalence of the two techniques. When the iodine atom was substituted by an  $\alpha$ -naphthyl group, two dynamic processes were observed. That with the lower barrier could be determined by NMR and that with the higher barrier by HPLC, thus outlining the complementarity of these two techniques.

## Introduction

Dynamic NMR spectroscopy gives valuable information concerning the conformational preferences and the internal motions of molecules in solution, also allowing the determination of the rate constants involved in the stereodynamic processes.<sup>2</sup> By applying this technique, some of us have recently determined the rotation barriers about the Ar–CN bond in a number of ortho-substituted aryl oxime derivatives.<sup>3</sup> This result prompted us to synthesize *O*-alkyl aryl oximes bearing ortho substituents of increasing dimension, so that dynamic NMR should be able to show whether the corresponding conformational antipodes (stereolabile atropisomers) might interconvert at a sufficiently slow rate as to allow their physical separation to be achieved by means of cryogenic enantioselective HPLC columns.

## Results and Discussion

*O*-alkyl benzyl aryl oximes bearing halogen atoms in the ortho position (**1–3** as in Chart 1) are expected to have the ortho-substituted phenyl ring significantly twisted with respect to the C=NO plane if the configuration *Z* is adopted. The corresponding dihedral angle ( $\theta$ ) has been computed (molecular mechanics calculations<sup>4</sup>) to be almost 90°, a situation which entails the

Chart 1

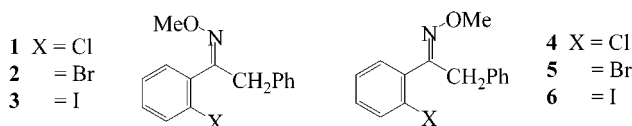
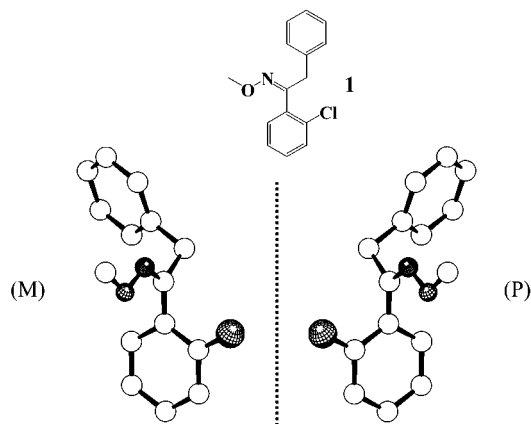


Chart 2. Computed<sup>4</sup> Structures of the M and P Atropisomers of **1** (X = Cl)



existence of M and P enantiomers (atropisomers) when the Ar–CN bond rotation rate is rendered sufficiently slow (Chart 2).

Experimental evidence of such an occurrence is offered by the <sup>1</sup>H NMR signals of the prochiral methylene group at low temperature. Whereas at ambient and higher temperatures these methylene hydrogens appear to be enantiotopic, yielding a single <sup>1</sup>H NMR line (see as an

<sup>†</sup> Università "La Sapienza".

<sup>‡</sup> University of Bologna.

<sup>§</sup> Università "G. D'Annunzio".

(1) Part 88: Bartoli, G.; Grilli, S.; Lunazzi, L.; Massaccesi, M.; Mazzanti, A.; Rinaldi, S. *J. Org. Chem.* **2002**, *67*, 2659–2664. (Web release March 23, 2002).

(2) Anderson, J. E.; de Meijere, A.; Kozhushkov, S. I.; Lunazzi, L.; Mazzanti, A. *J. Am. Chem. Soc.*, in press.

(3) Leardini, R.; Lunazzi, L.; Mazzanti, A.; McNab, H.; Nanni, D. *Eur. J. Org. Chem.* **2000**, 3439.

(4) MMX force field as implemented in the computer package PC Model, version 6, Serena Software, Bloomington, IN.

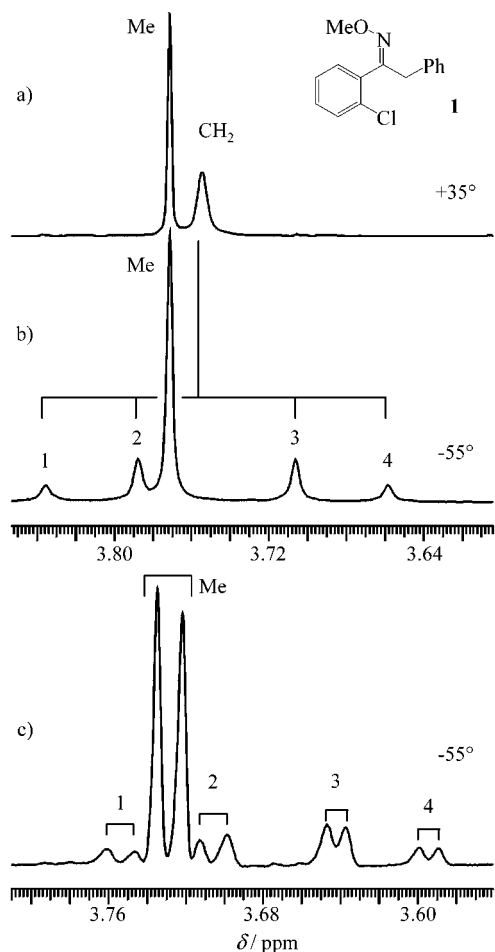


**Figure 1.** 300 MHz spectra of **1** ( $X = \text{Cl}$ ): (a) at  $+35\text{ }^\circ\text{C}$  displaying a single peak for both the methyl and methylene hydrogens; (b) at  $-55\text{ }^\circ\text{C}$  displaying a single peak for the methyl but displaying four lines for the methylene hydrogens (labeled as 1–4) of an AB-type spectrum ( $\Delta\nu = 35\text{ Hz}$ ,  $J = -14\text{ Hz}$ ); (c) in a chiral environment<sup>5</sup> two methyl lines and two AB-type spectra at  $-55\text{ }^\circ\text{C}$ , since the NMR signals of the two atropisomers of **1** are rendered anisochronous.

example Figure 1a for the case of **1**,  $X = \text{Cl}$ ), they become diastereotopic at lower temperatures (e.g. at  $-55\text{ }^\circ\text{C}$ ), consequently exhibiting the four-line pattern typical of an AB-type spectrum (Figure 1b).

Distinct NMR traces for the two atropisomers might be also observed, in principle, by acquiring the spectrum in a chiral environment at a temperature low enough as to make the interconversion rate negligible. Indeed, when an appropriate amount of an enantiopure chiral solvating agent (Pirkle's alcohol<sup>5</sup>) is introduced into the solution, two lines are observed for the methyl group and, likewise, two AB-type spectra for the methylene hydrogens of **1** at  $-55\text{ }^\circ\text{C}$  (Figure 1c).

That the anisochronicity of the methylene  $^1\text{H}$  signals observed in Figure 1b,c is actually a consequence of the restricted Ar–CN bond rotation is demonstrated by the failure to observe this feature in the corresponding *E* isomer **4** (Chart 1).

As the configuration *E* is less sterically hindered than the configuration *Z*, the corresponding Ar–CN rotation

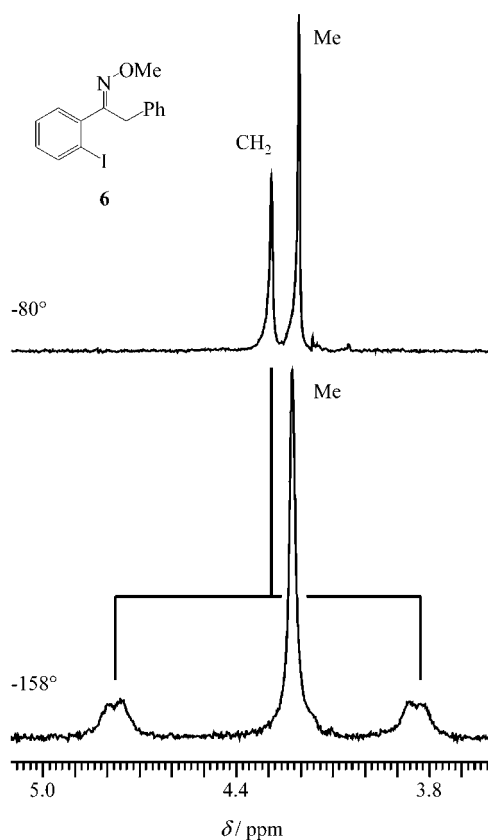


**Figure 2.**  $^1\text{H}$  spectrum (300 MHz) of the *E* isomer **6** at  $-80\text{ }^\circ\text{C}$  (top) and at  $-158\text{ }^\circ\text{C}$  (bottom), showing diastereotopic methylene hydrogens ( $\Delta\nu = 282\text{ Hz}$ ,  $J = -11\text{ Hz}$ ).

barrier is much lower, allowing a dynamically averaged plane of symmetry to be maintained at any attainable temperature, so that the methylene hydrogens of **4** appear always enantiotopic (not even at  $-160\text{ }^\circ\text{C}$  could anisochronous NMR signals be identified). In the case of the *E* isomer **6**, on the other hand, the dimension of the iodine substituent is sufficiently large as to allow detection of anisochronous methylene signals due to the slow interconversion of the corresponding atropisomers. The lesser steric requirements experienced by the configuration *E* is reflected, however, in the much lower temperature needed to observe such a phenomenon with respect to the corresponding iodine derivative in the configuration *Z* (compound **3**). Whereas the methylene hydrogens of the latter appear diastereotopic already at  $-5\text{ }^\circ\text{C}$ , those of **6** had to be cooled to  $-158\text{ }^\circ\text{C}$  to observe an AB-type spectrum, which displays a shift separation of 0.94 ppm and a geminal  $J$  coupling of  $-11\text{ Hz}$  (Figure 2). Line shape simulation<sup>6</sup> allowed us to determine the barrier for the interconversion of the atropisomers of **6** (enantiomerization process), which was as low as  $5.7 \pm 0.2\text{ kcal mol}^{-1}$ . In the more hindered *Z* isomers, the range of the  $\Delta G^\ddagger$  values for the enantiomerization process is obviously much higher (see entries **1–3** in Table 1) and, as conceivable, increase with the increasing dimensions of the ortho substituents (i.e. Cl, Br, I).

(5) The environment was rendered chiral by adding to the  $\text{CD}_2\text{Cl}_2$  solution of **1** a 3.6 M excess of (*R*)-1-(9-anthryl)-2,2,2-trifluoroethanol (see: Pirkle, W. H. *J. Am. Chem. Soc.* **1966**, *88*, 1837).

(6) Use was made of the program Auto-DNMR-y2k (Auto-Dynamic NMR), which is a PC version of the Program DNMR 6 (Binsch, G. et al., QCPE No. 633, Indiana University, Bloomington, IN) implemented with a Simplex algorithm for automatic fitting of the experimental data.

**Table 1.** NMR Measured Activation Free Energies ( $\Delta G^\ddagger$ ), Enthalpies ( $\Delta H^\ddagger$ ), and Entropies ( $\Delta S^\ddagger$ ) for the Aryl–CN Bond Rotation

	1	2	3	6	7	8≡2	9	10	11
$\Delta G^\ddagger$ <sup>c</sup>	12.6 ± 0.2	14.0 ± 0.2	15.9 ± 0.2	5.7 ± 0.2	13.9 ± 0.2	14.0 ± 0.2	13.9 ± 0.2	21.1 ± 0.2 <sup>a</sup>	12.7 ± 0.2 <sup>b</sup>
$\Delta H^\ddagger$ <sup>c</sup>	12.1 ± 0.9	14.3 ± 0.8	16.4 ± 1.	5.2 ± 0.5	14.4 ± 0.8	14.3 ± 0.8	14.2 ± 0.7	20.0 ± 1.2	12.7 ± 0.6
$\Delta S^\ddagger$ <sup>d</sup>	-2 ± 3	1 ± 2	2 ± 4	-4 ± 3	2 ± 3	1 ± 2	1 ± 2	-3 ± 4	0 ± 2

<sup>a</sup> Barrier to phenyl–naphthyl bond rotation. <sup>b</sup> The barrier to phenyl–naphthyl bond rotation (19.7<sub>5</sub> kcal mol<sup>-1</sup>) has been determined by cryogenic HPLC techniques (see text). <sup>c</sup> In kcal mol<sup>-1</sup>. <sup>d</sup> In cal mol<sup>-1</sup> T<sup>-1</sup>.

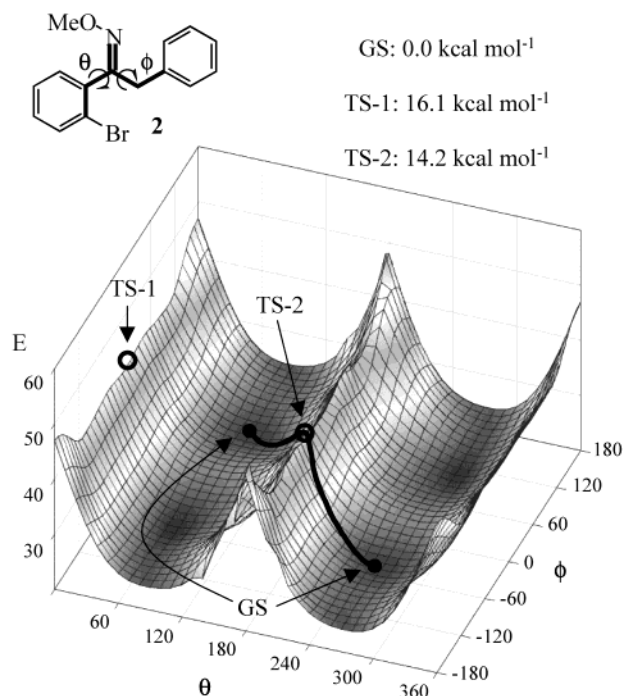


**Figure 3.** Computed<sup>4</sup> energy ( $E$  in kcal mol<sup>-1</sup>) surface of **2** ( $X = \text{Br}$ ) as a function of the Ar–CN ( $\theta$ ) and PhCH<sub>2</sub>–CN ( $\phi$ ) bond angles. The line of the lowest energy pathway to interconvert the P and M atropisomers corresponds to a transition state (TS-2) having  $\theta = 180^\circ$  and  $\phi = 0^\circ$ .

In principle two pathways are available to accomplish this process.

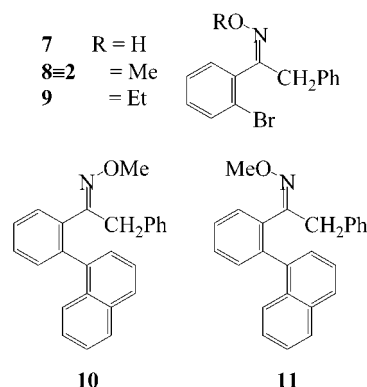
(i) The ortho halogen group might cross over the OMe moiety, leading to a transition state (TS-1) where the previously defined dihedral angle  $\theta$  is nearly  $0^\circ$ .

(ii) Alternatively, it might cross over the benzyl moiety, leading to a transition state (TS-2) where  $\theta$  is about  $180^\circ$ .

To choose between these two possibilities, the energy surface of **2** was computed (Figure 3) as a function of the dihedral angle  $\theta$  and of the dihedral angle between the C=NO and benzyl moieties ( $\phi$ ).<sup>7</sup> The barrier corresponding to the transition state TS-1 was found to be higher (16.1 kcal mol<sup>-1</sup>) than that corresponding to the transition state TS-2 (14.2 kcal mol<sup>-1</sup>). The lower value, in addition, coincides with the experimental result (14.0 kcal mol<sup>-1</sup>), thus strengthening the hypothesis that **2** (and conceivably also the analogous derivatives **1** and **3**) follows the TS-2 pathway to interconvert the two atropisomers.

A further support to this conclusion is offered by the determination of the enantiomerization barriers of the bromine derivatives **7–9** having the configuration Z (Chart 3).

(7) The barrier computed<sup>4</sup> for the PhCH<sub>2</sub>–CN bond rotation is too low (1.2 kcal mol<sup>-1</sup>) to affect the line shape of the NMR spectra.

**Chart 3**

As reported in Table 1, all these compounds have the same enantiomerization barriers: if the bromine substituent had crossed over the OR moiety, different barriers would have been observed, owing to the larger dimension of the R group in **9** ( $R = \text{Et}$ ) with respect to **8** ( $R = \text{Me}$ ) and to **7** ( $R = \text{H}$ ).

The invariance of the measured barriers agrees better with the pathway TS-2, where the bromine substituent crosses over the benzyl moiety, since the latter is kept unchanged along the series **7–9**. From the values of the free energy of activation reported in Table 1, it appears that the atropisomers of iodine derivative **3** have a relatively long half-life at temperatures close to  $-70^\circ\text{C}$ . This compound is therefore the best candidate for attempting a separation on a cryogenic enantioselective chromatographic column. The UV-detected HPLC signal of **3** actually broadens considerably below  $-40^\circ\text{C}$  and eventually splits into a pair of separated signals at  $-70^\circ\text{C}$  (Figure 4, left), corresponding to the M and the P enantiomers.<sup>8</sup> Similar to dynamic NMR analysis, peak shape simulation in chromatography provides quantitative kinetic information for on-column interconversion processes.<sup>9</sup> Computer simulation of the chromatographic profile (Figure 4, right) allowed us to obtain the rate constants for the exchange of the two atropisomers of **3**, from which the free energy of activation could be derived. The value obtained in this way ( $15.0 \pm 0.2$  kcal mol<sup>-1</sup>) is close to that independently determined by NMR ( $15.9 \pm 0.2$  kcal mol<sup>-1</sup>); part of the residual difference might arise from the need of using different solvents in the two methods.

(8) Casarini, D.; Lunazzi, L.; Pasquali, F.; Gasparrini, F.; Villani, C. *J. Am. Chem. Soc.* **1992**, *114*, 6521. Casarini, D.; Foresti, E.; Gasparrini, F.; Lunazzi, L.; Macciantelli, D.; Misiti, D.; Villani, C. *J. Org. Chem.* **1993**, *58*, 5674. Casarini, D.; Lunazzi, L.; Gasparrini, F.; Villani, C.; Cirilli, M.; Gavuzzo, E. *J. Org. Chem.* **1995**, *60*, 97.

(9) (a) Mannschreck, A.; Kiessl, L. *Chromatographia* **1989**, *28*, 263. Mannschreck, A.; Zinner, H.; Pustet, N. *Chimia* **1989**, *43*, 165. Stephan, B.; Zinner, H.; Kastner, F.; Mannschreck, A. *Chimia* **1990**, *44*, 336. (b) Jung, M.; Schurig, V. *J. Am. Chem. Soc.* **1992**, *114*, 529. Trapp, O.; Schurig, V. *J. Am. Chem. Soc.* **2000**, *122*, 1424. (c) Gasparrini, F.; Lunazzi, L.; Misiti, D.; Villani, C. *Acc. Chem. Res.* **1995**, *28*, 163. Casarini, D.; Lunazzi, L.; Alcaro, S.; Gasparrini, F.; Villani, C. *J. Org. Chem.* **1995**, *60*, 5515. Gasparrini, F.; Lunazzi, L.; Mazzanti, A.; Pierini, M.; Pietrusiewicz, K. M.; Villani, C. *J. Am. Chem. Soc.* **2000**, *122*, 4776.

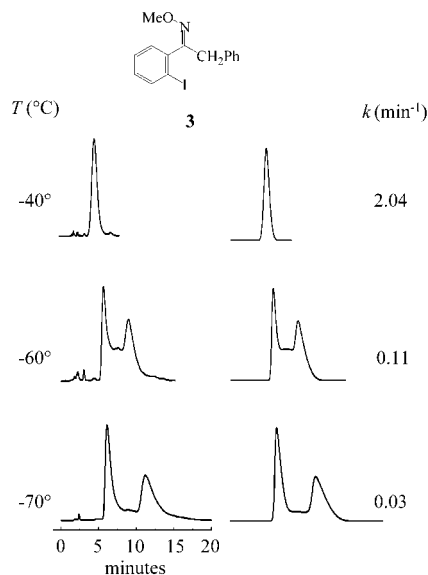


**Figure 4.** (left) Temperature-dependent chromatographic profiles (DHPLC) of **3** on a Chiralcel-OD column: experimental chromatograms (eluent *n*-hexane/IPA (98/2 v/v); flow rate 2.0 mL/min; UV detection 254 nm). (right) Computer simulation profile obtained with the rate constants reported for the on-column enantiomerization process.

If the halogen atoms in **1–6** are replaced by a bulky aromatic substituent such as the  $\alpha$ -naphthyl moiety, the resulting *E* and *Z* isomers (**10** and **11**, respectively, as in Chart 3) are expected to exhibit a substantial restriction about the phenyl–naphthyl bond. The presence of this second stereogenic axis should also generate a pair of atropisomers, in addition to those resulting from the restricted Ar–CN rotation.<sup>10</sup> Owing to the high rotation barrier about the phenyl–naphthyl bond, the <sup>1</sup>H methylene signals of **10** appear anisochronous even at ambient temperature, yielding the patterns of an AB spectrum typical for diastereotopic geminal hydrogens. When the temperature is raised, these lines broaden and coalesce at about +160 °C (see Experimental Section), displaying a barrier of 21.1 kcal mol<sup>-1</sup> for the interconversion of the mentioned atropisomers, due to the restriction of the phenyl–naphthyl rotation process.

This observation implies that, in the case of the more hindered *Z* isomer **11**, the restriction of the phenyl–naphthyl stereogenic axis, coupled with the restriction of the Ar–CN stereogenic axis, should allow the observation of two stereolabile diastereoisomers in a temperature range amenable to NMR detection. Each diastereoisomer also comprises a pair of atropisomers: the four species are displayed in Chart 4. Calculations predict the PP  $\equiv$  MM to be more stable than the PM  $\equiv$  MP diastereoisomer by 0.2 kcal mol<sup>-1</sup> (the dielectric constant of toluene as solvent has been considered in these calculations). Such an energy difference entails a relative proportion of the two stereolabile diastereoisomers equal to 62:38 at –55 °C, and the NMR spectrum of **11** at this temperature displays two groups of signals (Figure 5) in a similar ratio (in toluene-*d*<sub>8</sub> the equilibrium constant is 0.45; hence,  $\Delta G^\circ = 0.35$  kcal mol<sup>-1</sup>), in reasonable agreement with the expectations. On this basis the diastereoisomer

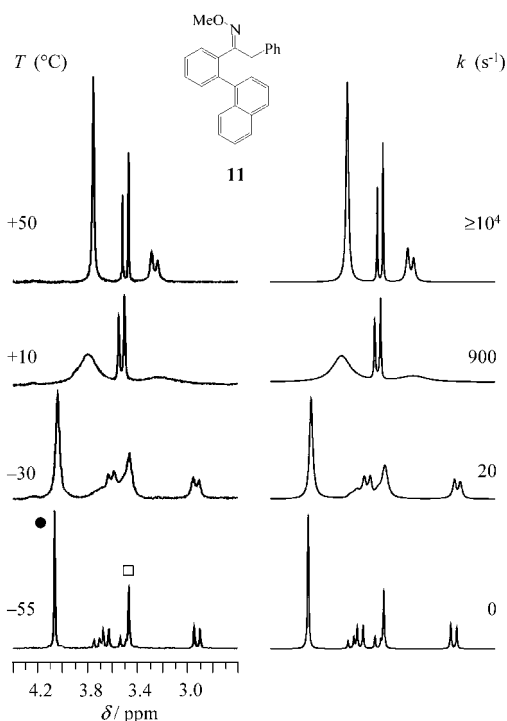
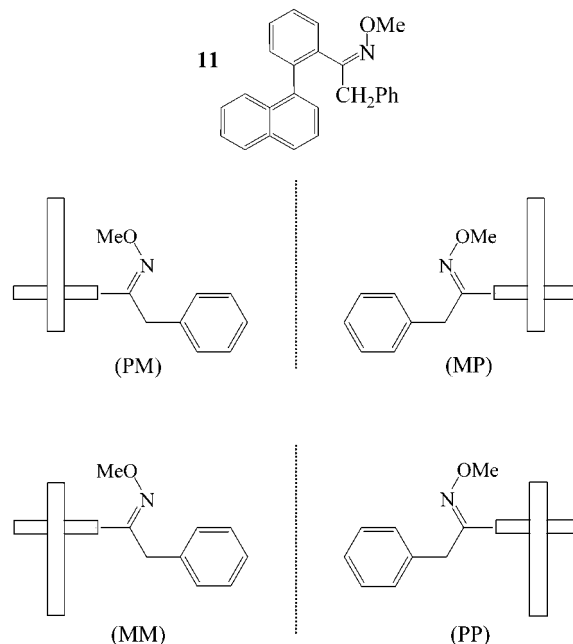


**Figure 5.** Experimental (left) and computer simulated (right) aliphatic region of the 300 MHz spectrum of the *Z* isomer **11** as function of temperature. In the trace at –55 °C the circle (●) identifies the Me signal of the major and the square (□) that of the minor diastereoisomer.

#### Chart 4. Representation of the Four Stereoisomers of **11** (*Z* Configuration)



corresponding to the PP and MM pair of enantiomers should be the one yielding the more intense NMR signal.

When the temperature is raised, the increased rotation rate about the Ar–CN axis interchanges the two diastereoisomers, so that at about +50 °C the spectrum due to an unique, averaged species is observed: the barrier corresponding to this process was found to be equal to 12.7 kcal mol<sup>-1</sup> (Table 1). The trace at +50 °C (Figure 5) still shows the pattern of an AB-type spectrum for the

(10) When the *E* isomers are involved, only in a single case (derivative **6**) could the spectral features due to the restricted Ar–CN rotation be actually detected, and this required a temperature as low as –158 °C (Figure 2).



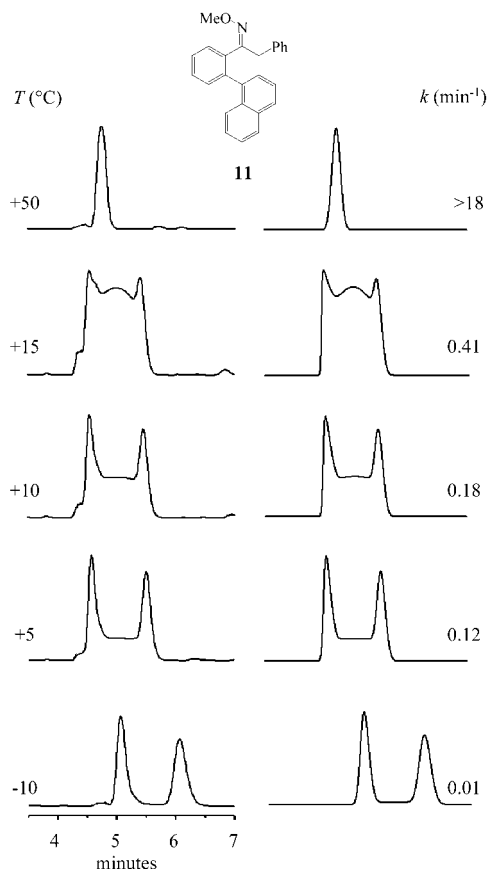


**Figure 6.** (left) Temperature-dependent chromatographic profiles (DHPLC) of **11** on a Chiralpak-AD column: experimental chromatograms (eluent *n*-hexane/IPA (98/2, v/v); flow rate 1.0 mL/min; UV detection 254 nm). (right) Computer simulation profile obtained with the rate constants reported for the on-column enantiomerization process.

methylene hydrogens, indicating that the phenyl–naphthyl rotation rate is not yet fast compared to the NMR time scale, as previously observed in the case of the *E* isomer **10**. In other words, we have determined only the lower of the two barriers in **11**, i.e., that corresponding to the interconversion of the two stereolabile diastereoisomers. To measure the higher barrier, which corresponds to the phenyl–naphthyl bond rotation, we should increase further the temperature. However, when the sample is warmed, the compound isomerizes rapidly into the *E* isomer **10**, making this determination impossible.

However, elution of **11** on an enantioselective column cooled to about  $-10$  °C allowed the separation of the atropisomers to be attained. This is because the time scale of the dynamic HPLC technique is longer than that of dynamic NMR and lower temperatures are required to slow the exchange of these two species. Consequently, the interconversion barrier due to phenyl–naphthyl bond rotation could be determined by HPLC in a temperature range quite lower than that of NMR, thus avoiding its interconversion into the *E* isomer **10** (Figure 6). The  $\Delta G^\ddagger$  value obtained in this way ( $19.7_5 \pm 0.2$  kcal mol $^{-1}$ ) is close to that previously measured for **10**, since in both cases the same type of motion is involved. In reasonable agreement with the experiment, computations<sup>4</sup> of the phenyl–naphthyl bond rotation processes yield barriers of 22.0 and 21.2 kcal mol $^{-1}$  for **10** and **11**, respectively.

Chromatographic separation of the conformational diastereoisomers of **11** could not be achieved since, as

mentioned, the longer time scale of this technique with respect to NMR would have required temperatures lower than  $-90$  °C to make these species sufficiently long-lived for HPLC detection. According to the NMR-measured barrier of 12.7 kcal mol $^{-1}$ , the half-life of the conformational diastereoisomers of **11** is in fact too short (only a few seconds) even at the lowest temperature ( $-70$  °C) attainable by our cryogenic HPLC apparatus.

Thus, dynamic NMR allowed the lower barrier, and dynamic HPLC the higher barrier, to be measured in the case of the *Z* isomer **11**: such an occurrence outlines the complementarity of the dynamic NMR and dynamic HPLC techniques.

## Experimental Section

**General Methods and Starting Materials.** Melting points are uncorrected.  $^1\text{H}$  and  $^{13}\text{C}$  NMR spectra were recorded in deuteriochloroform using tetramethylsilane or deuteriochloroform, respectively, as internal standards. Mass spectra (MS) were obtained by electron impact with a beam energy of 70 eV: relative intensities are given in parentheses. IR spectra were recorded in chloroform. Column chromatography was carried out on silica gel (ICN silica, 70–230 or 230–400 mesh) by gradual elution with light petroleum (40–70 °C)/diethyl ether (from 0 up to 100% diethyl ether) mixtures. Preparative tlc was performed on 1 mm thickness aluminum oxide plates by elution with a light petroleum (40–70 °C)/toluene (1:2.5) mixture. Organic phases were dried over magnesium sulfate.

Benzyl chloride, pyridinium chlorochromate, hydroxylamine hydrochloride, *O*-methylhydroxylamine hydrochloride, tetrakis(triphenylphosphine)palladium, bromoethane (Aldrich), and 1-naphthylboronic acid (Fluka) were commercially available. 1-(2-Chlorophenyl)-2-phenyl-1-ethanone,<sup>11</sup> 1-(2-bromophenyl)-2-phenyl-1-ethanone,<sup>12</sup> and 2-iodobenzaldehyde<sup>13</sup> were prepared according to the literature.

**1-(2-Iodophenyl)-2-phenyl-1-ethanol.** In a three-necked round-bottomed flask equipped with a mechanical stirrer, condenser, and dropping funnel a suspension of magnesium turnings (1.34 g, 55 mmol) in dry diethyl ether (100 mL) was treated dropwise at room temperature under nitrogen with benzyl chloride (6.95 g, 55 mmol). After the disappearance of magnesium, a solution of 2-iodobenzaldehyde (11.60 g, 50 mmol) in dry diethyl ether (50 mL) was added dropwise at 0 °C, and the resulting mixture was refluxed for 3 h. The final solution was hydrolyzed with water and extracted with diethyl ether. The organic phase was dried and the residue chromatographed to give the title compound (9.70 g, 60%) as a white solid: mp 90–91 °C;  $^1\text{H}$  NMR (200 MHz,  $\text{CDCl}_3$ ):  $\delta$  2.10 (br d,  $J = 2.3$  Hz, 1 H; OH), 2.67 (dd,  $J = 14.0, 9.3$  Hz, 1 H;  $\text{CH}_2$ ), 3.18 (dd,  $J = 14.0, 3.3$  Hz, 1 H;  $\text{CH}_2$ ), 5.05 (ddd,  $J = 9.3, 3.3, 2.3$  Hz, 1 H; CH), 6.97 (ddd,  $J = 7.1, 7.1, 2.0$  Hz, 1 H; Ar H), 7.20–7.42 (m, 6 H; Ar H), 7.56 (dd,  $J = 7.1, 1.8$  Hz, 1 H; Ar H), 7.81 (dd,  $J = 7.1, 1.6$  Hz, 1 H; Ar H);  $^{13}\text{C}$  NMR (50 MHz,  $\text{CDCl}_3$ )  $\delta$  45.12 ( $\text{CH}_2$ ), 79.10 (CHOH), 98.03 (C), 127.48 (CH), 127.68 (CH), 129.28 (CH), 129.92 (CH), 130.19 (CH), 138.72 (C), 139.94 (CH), 146.20 (C) (2 aromatic CH overlapped); IR ( $\text{CHCl}_3$ )  $\bar{\nu}$  3597, 3418, 3000, 1437, 1220, 1011  $\text{cm}^{-1}$ ; MS (70 eV)  $m/z$  (%) 324 (2) [ $M$ ] $^+$ , 233 (59), 232 (50), 105 (29), 92 (60), 91 (100). Anal. Calcd for  $\text{C}_{14}\text{H}_{13}\text{IO}$  (324.2): C, 51.87; H, 4.04. Found: C, 52.00; H, 4.05.

**1-(2-Iodophenyl)-2-phenyl-1-ethanone.** According to a reported procedure,<sup>14</sup> a solution of 1-(2-iodophenyl)-2-phenyl-1-ethanol (3.07 g, 9.48 mmol) in dichloromethane (10 mL) was rapidly added at room temperature and with magnetic stirring to a mixture of pyridinium chlorochromate (3.07 g, 14.22 mmol) and dichloromethane (20 mL). After 3 h, the mixture was

(11) Newman, M. S.; Reid, D. E. *J. Org. Chem.* **1958**, *23*, 665.

(12) Koral, M.; Becker, E. I. *J. Org. Chem.* **1962**, *27*, 1038.

(13) Berry, J. M.; Watson, C. I.; Whish, W. J. D.; Threadgill, M. D. *J. Chem. Soc., Perkin Trans. 1* **1997**, 1147.

(14) Corey, E. J.; Suggs, J. W. *Tetrahedron Lett.* **1975**, 2647.

diluted with dry diethyl ether (150 mL) and filtered. The filtrate was evaporated and the residue chromatographed to give the title compound (2.41, 79%) as a thick oil:  $^1\text{H NMR}$  (200 MHz,  $\text{CDCl}_3$ )  $\delta$  4.20 (s, 2 H;  $\text{CH}_2$ ), 7.05–7.17 (m, 1 H; Ar *H*), 7.20–7.40 (m, 7 H; Ar *H*), 7.90 (d,  $J = 7.5$  Hz, 1 H; Ar *H*);  $^{13}\text{C NMR}$  (50 MHz,  $\text{CDCl}_3$ )  $\delta$  48.69 ( $\text{CH}_2$ ), 91.12 (C), 127.02 (CH), 127.85 (CH), 128.52 (CH), 129.62 (CH), 131.42 (CH), 133.23 (C), 140.27 (CH), 144.18 (C), 201.86 (C) (2 aromatic CH overlapped); IR (film)  $\tilde{\nu}$  3000, 1696  $\text{cm}^{-1}$ ; MS (70 eV)  $m/z$  (%) 322 (7)  $[M]^+$ , 231 (100), 203 (34), 104 (13), 91 (44), 76 (76). Anal. Calcd for  $\text{C}_{14}\text{H}_{11}\text{IO}$  (322.1): C, 52.20; H, 3.44. Found: C, 52.30; H, 3.43.

#### General Procedure for the Preparation of Oximes.<sup>15</sup>

A mixture of the ketone (10 mmol) and hydroxylamine hydrochloride (for oxime 7) or *O*-methylhydroxylamine hydrochloride (for oximes 1–6, 10, and 11) (15 mmol) in pyridine (2.5 mL)/ethanol (25 mL) was refluxed for 3–4 h. The solvent was evaporated and the residue repeatedly chromatographed, as described for each compound, to separate the *E* and *Z* isomers.

**(Z)-1-(2-Bromophenyl)-2-phenyl-1-ethanone Oxime (7)** and **(E)-1-(2-Bromophenyl)-2-phenyl-1-ethanone Oxime**: eluent light petroleum (40–70 °C)/diethyl ether (98:2 v/v); yield 97%; *E/Z* ratio 55:45; MS (70 eV) (*E + Z*)  $m/z$  (%): 391 (12)  $[M + 2]^+$ , 289 (11)  $[M]^+$ , 273 (16), 271 (15), 210 (8), 91 (100). Anal. Calcd for  $\text{C}_{14}\text{H}_{12}\text{BrNO}$  (290.2) (*E + Z*): C, 57.95; H, 4.16; N, 4.82. Found C, 58.15; H, 4.17; N, 4.83. *E* isomer: mp 120–123 °C (from light petroleum/benzene);  $^1\text{H NMR}$  (200 MHz,  $\text{CDCl}_3$ )  $\delta$  4.05 (s, 2 H;  $\text{CH}_2$ ), 6.85–6.95 (m, 1 H; Ar *H*), 6.95–7.20 (m, 7 H; Ar *H*), 7.40–7.50 (m, 1 H; Ar *H*), 9.28 (br s, 1 H; OH);  $^{13}\text{C NMR}$  (50 MHz,  $\text{CDCl}_3$ )  $\delta$  35.64 ( $\text{CH}_2$ ), 122.75 (C), 127.13 (CH), 127.75 (CH), 129.01 (CH), 130.09 (CH), 130.74 (CH), 131.85 (CH), 133.60 (CH), 136.25 (C), 137.67 (C), 159.84 (C); IR ( $\text{CHCl}_3$ )  $\tilde{\nu}$  3580, 3311, 3000, 1450, 1025  $\text{cm}^{-1}$ . *Z* isomer (7): mp 91.3–92.5 °C (from light petroleum/benzene);  $^1\text{H NMR}$  (200 MHz,  $\text{CDCl}_3$ )  $\delta$  3.75 (br s, 2 H;  $\text{CH}_2$ ), 6.55–6.70 (m, 1 H; Ar *H*), 7.00–7.20 (m, 7 H; Ar *H*), 7.45–7.55 (m, 1 H; Ar *H*), 8.92 (br s, 1 H; OH);  $^{13}\text{C NMR}$  (50 MHz,  $\text{CDCl}_3$ )  $\delta$  41.86 ( $\text{CH}_2$ ), 120.96 (C), 127.50 (CH), 129.04 (CH), 129.93 (CH), 130.20 (CH), 130.47 (CH), 133.20 (CH), 136.10 (C), 158.33 (C) (2 CH overlapped and 1 C nonvisible); IR ( $\text{CHCl}_3$ )  $\tilde{\nu}$  3575, 3318, 3000, 1450, 1220, 1025  $\text{cm}^{-1}$ .

**(Z)-1-(2-Chlorophenyl)-2-phenyl-1-ethanone *O*-Methyl-oxime (1)** and **(E)-1-(2-Chlorophenyl)-2-phenyl-1-ethanone *O*-Methyl-oxime (4)**: eluent light petroleum (40–70 °C)/toluene (30:70 v/v); yield 73%; *E/Z* ratio 66:34; MS (70 eV) (*E + Z*)  $m/z$  (%) 261 (3)  $[M + 2]^+$ , 259 (8)  $[M]^+$ , 229 (36), 227 (100), 192 (9), 168 (8), 153 (22), 91 (82). Anal. Calcd for  $\text{C}_{15}\text{H}_{14}\text{ClNO}$  (259.7) (*E + Z*): C, 69.36; H, 5.43; N, 5.39. Found: C, 69.55; H, 5.41; N, 5.37. *E* isomer (4): oil;  $^1\text{H NMR}$  (200 MHz,  $\text{CDCl}_3$ )  $\delta$  3.92 (s, 3 H;  $\text{OCH}_3$ ), 4.05 (s, 2 H;  $\text{CH}_2$ ), 6.90–7.30 (m, 9 H; Ar *H*);  $^{13}\text{C NMR}$  (50 MHz,  $\text{CDCl}_3$ )  $\delta$  36.00 ( $\text{CH}_2$ ), 62.61 ( $\text{CH}_3$ ), 126.99 (CH), 127.17 (CH), 128.94 (CH), 129.87 (CH), 130.32 (CH), 130.44 (CH), 131.82 (CH), 133.32 (C), 135.87 (C), 136.47 (C), 158.11 (C); IR (film)  $\tilde{\nu}$  3000, 1433, 1045  $\text{cm}^{-1}$ . *Z* isomer (1): oil;  $^1\text{H NMR}$  (200 MHz,  $\text{CDCl}_3$ )  $\delta$  3.73 (s, 2 H;  $\text{CH}_2$ ), 3.80 (s, 3 H;  $\text{OCH}_3$ ), 6.59 (dd,  $J = 7.5, 1.8$  Hz, 1 H; Ar *H*), 6.95–7.18 (m, 7 H; Ar *H*), 7.27 (dd,  $J = 8.0, 1.4$  Hz, 1 H; Ar *H*);  $^{13}\text{C NMR}$  (50 MHz,  $\text{CDCl}_3$ )  $\delta$  41.92 ( $\text{CH}_2$ ), 62.64 ( $\text{CH}_3$ ), 126.82 (CH), 127.41 (CH), 128.99 (CH), 129.69 (CH), 129.95 (CH), 130.09 (CH), 131.80 (C), 134.41 (C), 136.44 (C), 155.86 (C) (2 aromatic CH overlapped); IR (film)  $\tilde{\nu}$  3000, 1450, 1058, 1022  $\text{cm}^{-1}$ . An NOE experiment (400 MHz, toluene- $d_6$ ) was carried out on the *E/Z* mixture by irradiating the methylene signal that is independent of the temperature (4.17 ppm). Since only the *E* isomer could experience a positive NOE effect between the methylene and the methoxy group, the observed outcome (2%) on the (*E*)-OMe group (3.85 ppm) confirmed that the (*E*)-oxime is not responsible for the observed splitting of the signals as function of temperature.

**(Z)-1-(2-Bromophenyl)-2-phenyl-1-ethanone *O*-Methyl-oxime (2)** and **(E)-1-(2-Bromophenyl)-2-phenyl-1-etha-**

**none *O*-Methyl-oxime (5)**: yield 75%; *E/Z* ratio 69:31; pure samples of the *Z* isomer (2) could not be obtained by any kind of chromatography, even by preparative tlc. The spectral data reported below for 2 were recorded with a sample of the pure (*Z*)-oxime obtained by kinetic resolution as a residue of the Suzuki arylation of 2 to give the naphthyl derivatives 10 and 11. MS (70 eV) (*E + Z*):  $m/z$  (%) 305 (3)  $[M + 2]^+$ , 303 (4)  $[M]^+$ , 273 (35), 271 (37), 199 (10), 197 (10), 91 (100). Anal. Calcd for  $\text{C}_{15}\text{H}_{14}\text{BrNO}$  (304.2) (*E + Z*): C, 59.22; H, 4.63; N, 4.60. Found: C, 59.30; H, 4.62; N, 4.62. *E* isomer (5): oil;  $^1\text{H NMR}$  (200 MHz,  $\text{CDCl}_3$ )  $\delta$  3.99 (s, 3 H;  $\text{OCH}_3$ ), 4.10 (s, 2 H;  $\text{CH}_2$ ), 6.90–7.00 (m, 1 H; Ar *H*), 7.05–7.22 (m, 7 H; Ar *H*), 7.47–7.54 (m, 1 H; Ar *H*);  $^{13}\text{C NMR}$  (75 MHz,  $\text{CDCl}_3$ )  $\delta$  36.24 ( $\text{CH}_2$ ), 62.67 ( $\text{CH}_3$ ), 122.83 (C), 127.06 (CH), 127.74 (CH), 129.00 (CH), 130.02 (CH), 130.62 (CH), 131.96 (CH), 133.53 (CH), 136.42 (C), 137.82 (C), 159.12 (C); IR (film)  $\tilde{\nu}$  3000, 1430, 1045  $\text{cm}^{-1}$ . *Z* isomer (2): oil;  $^1\text{H NMR}$  (300 MHz,  $\text{CDCl}_3$ )  $\delta$  3.80 (br s, 2 H;  $\text{CH}_2$ ), 3.85 (s, 3 H;  $\text{OCH}_3$ ), 6.55–6.65 (m, 1 H; Ar *H*), 7.05–7.15 (m, 4 H; Ar *H*), 7.15–7.25 (m, 3 H; Ar *H*), 7.50–7.60 (m, 1 H; Ar *H*);  $^{13}\text{C NMR}$  (75 MHz,  $\text{CDCl}_3$ )  $\delta$  41.92 ( $\text{CH}_2$ ), 62.69 ( $\text{CH}_3$ ), 121.02 (C), 127.40 (CH), 127.47 (CH), 129.02 (CH), 129.83 (CH), 130.22 (CH), 133.11 (CH), 136.42 (C), 136.67 (C), 156.92 (C) (2 aromatic CH overlapped); IR (film)  $\tilde{\nu}$  3000, 1460, 1051, 1019  $\text{cm}^{-1}$ .

**(Z)-1-(2-Iodophenyl)-2-phenyl-1-ethanone *O*-Methyl-oxime (3)** and **(E)-1-(2-Iodophenyl)-2-phenyl-1-ethanone *O*-Methyl-oxime (6)**: preparative tlc, eluent light petroleum (40–70 °C)/toluene (30:70 v/v); yield 69%; *E/Z* ratio 75:25; MS (70 eV) (*E + Z*)  $m/z$  (%) 351 (44)  $[M]^+$ , 319 (66), 260 (9), 245 (20), 229 (13), 192 (12), 91 (100). Anal. Calcd for  $\text{C}_{15}\text{H}_{14}\text{INO}$  (351.2) (*E + Z*): C, 51.30; H, 4.02; N, 3.99. Found: C, 51.40; H, 4.01; N, 3.99. *E* isomer (6): oil;  $^1\text{H NMR}$  (300 MHz,  $\text{CDCl}_3$ )  $\delta$  4.03 (s, 3 H;  $\text{OCH}_3$ ), 4.07 (s, 2 H;  $\text{CH}_2$ ), 6.88 (d,  $J = 8.0$  Hz, 1 H; Ar *H*), 6.92–7.00 (m, 1 H; Ar *H*), 7.10–7.25 (m, 6 H; Ar *H*), 7.82 (d,  $J = 7.5$  Hz, 1 H; Ar *H*);  $^{13}\text{C NMR}$  (50 MHz,  $\text{CDCl}_3$ )  $\delta$  36.51 ( $\text{CH}_2$ ), 62.64 ( $\text{CH}_3$ ), 97.53 (C), 127.10 (CH), 128.39 (CH), 129.00 (CH), 130.12 (CH), 130.53 (CH), 131.13 (CH), 136.22 (C), 139.94 (CH), 141.47 (C), 160.52 (C); IR (film)  $\tilde{\nu}$  3000, 1430, 1042  $\text{cm}^{-1}$ . *Z* isomer (3): oil;  $^1\text{H NMR}$  (300 MHz,  $\text{CDCl}_3$ )  $\delta$  3.80 (AB,  $J = 14.2$  Hz,  $\Delta\nu = 57.4$  Hz, 2 H;  $\text{CH}_2$ ), 3.86 (s, 3 H;  $\text{OCH}_3$ ), 6.50 (dd,  $J = 7.6, 1.4$  Hz, 1 H; Ar *H*), 6.94 (ddd,  $J = 8.0, 8.0, 1.6$  Hz, 1 H; Ar *H*), 7.08–7.29 (m, 6 H; Ar *H*), 7.80 (d,  $J = 8.0$  Hz, 1 H; Ar *H*);  $^{13}\text{C NMR}$  (75 MHz,  $\text{CDCl}_3$ )  $\delta$  41.96 ( $\text{CH}_2$ ), 62.67 ( $\text{CH}_3$ ), 95.38 (C), 127.46 (CH), 128.10 (CH), 129.01 (CH), 129.19 (CH), 130.12 (CH), 130.31 (CH), 136.34 (C), 139.49 (CH), 141.16 (C), 158.72 (C); IR (film)  $\tilde{\nu}$  3000, 1430, 1047  $\text{cm}^{-1}$ .

**(Z)-1-(2-Bromophenyl)-2-phenyl-1-ethanone *O*-Ethyl-oxime (9)**. A mixture of the (*Z*)-oxime 7 (0.23 g, 0.8 mmol), bromoethane (1.13 g, 1.2 mmol), and potassium carbonate (0.8 g, 5.8 mmol) in DMSO (30 mL) was kept at 55 °C in a sealed Pyrex tube with magnetic stirring for 12 h. The final mixture was poured into water and extracted with diethyl ether. The organic phase was dried, the solvent was evaporated, and the residue was chromatographed to give the pure (*Z*)-oxime 9 as an oil (0.08 g, 30%);  $^1\text{H NMR}$  (200 MHz,  $\text{CDCl}_3$ )  $\delta$  1.15 (t,  $J = 7.2$  Hz, 3 H;  $\text{OCH}_2\text{CH}_3$ ), 3.73 (vbr s, 2 H;  $\text{PhCH}_2$ ), 4.05 (q,  $J = 7.2$  Hz, 2 H;  $\text{OCH}_2\text{CH}_3$ ), 6.46–6.56 (m, 1 H; Ar *H*), 7.00–7.20 (m, 7 H; Ar *H*), 7.42–7.52 (m, 1 H; Ar *H*);  $^{13}\text{C NMR}$  (75 MHz,  $\text{CDCl}_3$ )  $\delta$  15.51 ( $\text{CH}_3$ ), 42.05 ( $\text{PhCH}_2$ ), 70.30 ( $\text{OCH}_2$ ), 121.08 (C), 127.33 (CH), 127.38 (CH), 128.98 (CH), 129.92 (CH), 130.08 (CH), 130.21 (CH), 133.08 (CH), 133.56 (C), 136.70 (C), 156.57 (C); MS (70 eV)  $m/z$  (%) 319 (1)  $[M + 2]^+$ , 317 (1)  $[M]^+$ , 273 (17), 271 (18), 91 (100). Anal. Calcd for  $\text{C}_{16}\text{H}_{16}\text{BrNO}$  (318.2): C, 60.39; H, 5.06; N, 4.40. Found: C, 60.57; H, 5.08; N, 4.39.

**(E)-1-[2-(1-Naphthyl)phenyl]-2-phenyl-1-ethanone *O*-Methyl-oxime (10)** and **(Z)-1-[2-(1-Naphthyl)phenyl]-2-phenyl-1-ethanone *O*-Methyl-oxime (11)**. According to a reported procedure,<sup>16</sup> a benzene (11 mL) solution of oximes 2 and 5 (ca. 1:1, 0.53 g, 1.75 mmol overall amount) was treated

(15) Vogel, A. I. *Practical Organic Chemistry*, 4th ed.; Longmans: London, 1969; p 345.

(16) Miyaura, N.; Yamagi, T.; Suzuki, A. *Synth. Commun.* **1981**, *11*, 513.

at ambient temperature with an aqueous 2 M solution of potassium carbonate (1.75 mL); an ethanol (4 mL) solution of 1-naphthylboronic acid (0.33 g, 1.9 mmol) was added, followed by tetrakis(triphenylphosphine)palladium(0) (0.12 g, 0.1 mmol), and the resulting mixture was refluxed for 5 h. The final mixture was diluted with water and extracted with diethyl ether. The organic phase was separated and dried. After evaporation of the solvent, the residue was chromatographed to give ca. 0.1 g of the starting oxime **2** together with a 57:43 mixture of the title compounds (0.28 g, 46% overall yield). Preparative tlc with light petroleum (40–70 °C)/toluene (30:70 v/v) allowed separation of the geometric isomers: MS (70 eV) (*E* + *Z*) *m/z* (%) 351 (94) [*M*]<sup>+</sup>, 320 (100), 260 (12), 229 (37), 228 (55), 215 (33), 202 (25), 91 (70). Anal. Calcd for C<sub>25</sub>H<sub>21</sub>NO (351.4) (*E* + *Z*): C, 85.44, H, 6.02; N, 3.98. Found: C, 85.70; H, 6.04; N, 3.99; *E* isomer (**10**): oil; <sup>1</sup>H NMR (200 MHz, CDCl<sub>3</sub>) δ 3.12 (AB, *J* = 13.8 Hz, Δ*v* = 121.5 Hz, 2 H; *CH*<sub>2</sub>), 3.73 (s, 3 H; *OCH*<sub>3</sub>), 6.67–6.78 (m, 2 H; Ar *H*), 6.95–7.10 (m, 3 H; Ar *H*), 7.20–7.50 (m, 8 H; Ar *H*), 7.62 (d, *J* = 8.1 Hz, 1 H; Ar *H*), 7.75–7.85 (m, 2 H; Ar *H*); <sup>13</sup>C NMR (50 MHz, CDCl<sub>3</sub>) δ 35.32 (CH<sub>2</sub>), 62.28 (CH<sub>3</sub>), 125.87 (CH), 126.51 (CH), 126.64 (CH), 126.68 (CH), 127.14 (CH), 128.24 (CH), 128.46 (CH), 128.55 (CH), 128.75 (CH), 129.02 (CH), 129.55 (CH), 130.91 (CH), 132.19 (CH), 132.51 (C), 134.27 (C), 136.86 (C), 137.16 (C), 139.08 (C), 139.46 (C), 159.96 (C) (2 aromatic CH overlapped); IR (CHCl<sub>3</sub>)  $\tilde{\nu}$  3000, 1262, 1049 cm<sup>-1</sup>. *Z* isomer (**11**): oil; <sup>1</sup>H NMR (200 MHz, toluene-*d*<sub>6</sub>) δ 3.21 (vbr s, A part of AB, 1 H; *CH*<sub>2</sub>), 3.48 (d, B part of AB, *J* = 14.2 Hz, 1 H; *CH*<sub>2</sub>), 3.75 (vbr s, 3 H; *OCH*<sub>3</sub>), 6.60–6.75 (m, 8 H; Ar *H*), 6.90–7.04 (m, 5 H; Ar *H*), 7.32–7.42 (m, 2 H; Ar *H*), 7.57–7.65 (m, 1 H; Ar *H*); IR (film)  $\tilde{\nu}$  3000, 1262, 1099, 1023 cm<sup>-1</sup>.

**Chromatography.** Chiralcel-OD (cellulose tris(3,5-dimethyl phenylcarbamate) coated on a 5 μm macroporous silica gel) and Chiralpak-AD (amylose tris(3,5-dimethyl phenylcarbamate) coated on a 5 μm macroporous silica gel) columns (25 × 0.46 cm) were obtained from Chiral Technologies (Exton, PA). Variable-temperature chromatography with UV detection<sup>9c</sup>

and low-temperature chromatography were performed by placing the column inside a thermally insulated container cooled by the expansion of liquid carbon dioxide. The flow of liquid CO<sub>2</sub> and the column temperature are regulated by a solenoid valve, a thermocouple, and an electronic controller. Temperature variations after thermal equilibration are within ±0.5 °C. Computer simulation<sup>17</sup> of the experimental chromatograms was performed as previously described.<sup>9c</sup>

**NMR Measurements.** The variable-temperature spectra were obtained in toluene-*d*<sub>8</sub> solutions, except for compounds **10** (in hexachloroacetone/C<sub>6</sub>D<sub>6</sub>) and **6**. In the latter case the sample was prepared by connecting to a vacuum line the NMR tubes containing the compound and some C<sub>6</sub>D<sub>6</sub> for locking purposes and condensing therein the gaseous solvents (CHF<sub>2</sub>-Cl and CHFCl<sub>2</sub> in a 4:1 v/v ratio) under cooling with liquid nitrogen. The tube was subsequently sealed in vacuo and introduced into the precooled probe of the 300 MHz spectrometer (Varian, Gemini). The temperatures were calibrated by substituting the samples with a precision Cu/Ni thermocouple before the measurements.

**Acknowledgment.** Financial support has been received from MURST (national project “Stereoselection in Organic Synthesis”) and from the University of Bologna (Funds for selected research topics 1999–2001). F.G. also acknowledges financial support from the University “La Sapienza”, Roma (Finanziamento Ricerche di Ateneo 2001–2003).

JO0255431

(17) Use was made of the program Auto-DHPLC-y2k (Auto-Dynamic HPLC), which is an improved version for PC of the Program SIMUL (M. Jung, QCPE No. 620, Indiana University, Bloomington, IN) implemented with a Simplex algorithm for automatic fitting of experimental data.